Published in final edited form as:
*J Heart Valve Dis*. 2012 March ; 21(2): 247–252.

# An Ovine Model of Pulmonary Insufficiency and Right Ventricular Outflow Tract Dilatation

**J. Daniel Robb**[2], **Matthew A. Harris**[1], **Masahito Minakawa**[2], **Evelio Rodriguez**[3], **Kevin J. Koomalsingh**[2], **Takashi Shuto**[2], **Yoav Dori**[1], **Robert C. Gorman**[2], **Joseph H. Gorman III**[2], and **Matthew J. Gillespie**[1,2]

[1]Department of Pediatric Cardiology, Children's Hospital of Philadelphia, Philadelphia, Pennsylvania

[2]Gorman Cardiovascular Research Group, University of Pennsylvania, Glenolden, Pennsylvania

[3]Department of Surgery, East Carolina University, Greenville, North Carolina, USA

## Abstract

**Background and aim of the study—**The treatment of pulmonary insufficiency (PI) following reconstructive surgery of the right ventricular outflow tract (RVOT) in repair of the tetralogy of Fallot remains a significant challenge. The study aim was to establish an ovine model of dilated RVOT and PI, and to quantify the degree of PI and right ventricular remodeling over an eight-week period, using magnetic resonance imaging (MRI).

**Methods—**Five sheep underwent baseline MRI scanning and catheterization. The weight-indexed right and left ventricular end-diastolic volume (EDV), end-systolic volume (ESV), stroke volume (SV), ejection fraction (EF) and pulmonary regurgitant fraction (RF) were measured at baseline. The animals then underwent pulmonary valvectomy and transannular patch repair of the RVOT. Repeat MRI and hemodynamic measurements were obtained after an eight-week period.

**Results—**The indexed RVEDV increased from 49 ± 4.0 ml/m$^2$ at baseline to 80 ± 10.3 ml/m$^2$ at eight weeks after valvectomy ($p = 0.01$), while the indexed RVESV increased from 13 ± 3.4 ml/m$^2$ to 33 ± 8.8 ml/m$^2$ ($p = 0.01$). The indexed RVSV increased from 36 ± 3.7 ml/m$^2$ to 47 ± 1.7 ml/m$^2$ ($p = 0.01$). The RVEF at baseline was 74 ± 6%, and this decreased to 59 ± 5% at follow up ($p = 0.02$). The RF at baseline was 0 ± 0% and was increased to 37 ± 3% at eight weeks after valvectomy ($p < 0.001$). The left ventricular (LV) function was also diminished: LVEF at baseline was 67 ± 2%, versus 49 ± 10% at follow up ($p = 0.01$). Both, the RV and LV end-diastolic pressures were significantly elevated at follow up.

**Conclusion—**All five animals developed pulmonary regurgitation sufficient to cause significant RV dilatation and diminished RV and LV functions. This model may be used to investigate novel therapeutic approaches in the treatment of this difficult clinical problem.



Address for correspondence: Robert C. Gorman MD, Gorman Cardiovascular Research Group, Glenolden Research Laboratory, University of Pennsylvania, 500 S. Ridgeway Avenue, Glenolden, PA 19036, USA, gormanr@uphs.upenn.edu.

The treatment of patients with pulmonary insufficiency (PI) following reconstructive surgery of the right ventricular outflow tract (RVOT) for congenital heart disease remains an important clinical challenge. Longstanding PI typically leads to right ventricular (RV) dilatation, exercise intolerance, ventricular arrhythmias, and heart failure. This adverse remodeling of the right ventricle is a common indication for late reintervention following surgical repair of the tetralogy of Fallot (ToF) (1-10).

A homograft conduit or bioprosthetic valve replacement are commonly used for the surgical treatment of RVOT dysfunction (11) although, due to their tendency to degenerate and calcify, these prostheses often fail very quickly. Such concern over prosthesis longevity frequently delays the decision to refer patients for surgery, thereby subjecting them to ongoing PI and the risk of irreversible RV damage. This clinical dilemma has led to the development of minimally invasive approaches to PI following RVOT reconstruction for congenital heart disease.

The first implantation of a transcatheter pulmonary valve in animals, and subsequently in humans, was made in 2000 (12,13). Yet, increasing experience with transcatheter pulmonary valve placement has demonstrated the benefits and limitations of this therapy (1,14-21). It has been shown that the percutaneous implantation of valved stents in failed right ventricle to pulmonary artery (PA) conduits represents an effective means of rehabilitating a surgically placed homograft. The patients benefit in both the short and medium terms, with improvements in symptoms, aerobic and anaerobic exercise capacity, RV volumes and systolic and diastolic function, without incurring the risk of open-heart surgery (18,22-24).

Percutaneous pulmonary valve replacement does, however, have certain limitations, with the use of this technique generally having been limited to ‘conduit rehabilitation’. Currently available devices - namely, the Melody® valve (Medtronic, Minneapolis, MN, USA) and the SAPIEN® valve (Edwards Lifesciences, Irvine, CA, USA) - have maximum functional diameters of 22 mm and 26 mm, respectively, and are therefore not suitable for dilated RVOTs (21). Unfortunately, massively dilated RVOTs are commonly encountered in clinical practice, particularly in patients who have undergone transannular patch repair of ToF. Although attempts have been made to downsize the large outflow tracts - either surgically, or with a filler device to facilitate valved-stent deployment (16,25) - these procedures have met with only limited success. In addition, the RVOT is often not only dilated but also highly asymmetrical and distorted, which makes the placement of any device difficult. Thus, a dilated and distorted RVOT remains a considerable clinical challenge, and provides a fertile area for study.

In order to permit laboratory investigations of this important clinical problem, an ovine model of pulmonary valve insufficiency with a dilated RVOT has been developed that closely replicates the common late clinical presentation for ToF patients who previously would have been treated with a transannular patch.

## Materials and methods

### Baseline magnetic resonance imaging (MRI) study

Five female Dorsett hybrid sheep (body weight 50-83 kg) were used in these studies. Following the induction of anesthesia with sodium thiopental (10-15 mg/kg, intravenously), each animal was intubated endotracheally and the anesthesia maintained with 1-2% isoflurane in oxygen. All animals received glycopyrrolate (0.02 mg/kg intravenously) to minimize secretions associated with endotracheal intubation. During the operative procedure, a surface electrocardiogram and arterial blood pressure were monitored continuously. A 9F central venous catheter and a pulmonary artery catheter (131h-7F; Baxter Healthcare, Irvine, CA, USA) were placed to monitor temperature and hemodynamics, and to measure the right-sided cardiac pressures. The pulmonary catheter was removed prior to MRI scanning. A high-fidelity pressure transducer (SPC-350; Millar Instruments, Inc., Houston, TX, USA) was passed percutaneously via the femoral artery into the left ventricle, so as to allow continuous left ventricular (LV) pressure monitoring, as well as facilitating the gating of the subsequent image acquisition in the MRI scanner.

On completion of instrumentation, the animals were transferred to the MRI scanner for cardiac imaging. All scans were performed using a 3T Siemens Avanto scanner (Siemens Corp., New York, USA). Following the MRI investigations, the animals were allowed to recover and then returned to their housing units.

The animal studies were conducted in compliance with the *Guide for the Care and Use of Laboratory Animals* (National Institutes of Health Publication no 85-23, revised 1996), and under an experimental protocol approved by The University of Pennsylvania's Institute of Animal Care and Use Committee.

### Pulmonary valvectomy and transannular patch surgery

After one to two weeks, each animals was re-anesthetized as described above, and a left thoracotomy performed to expose the RVOT/pulmonary artery. An oval Gore-Tex® patch (Gore-Tex® Acuseal Cardiovascular Patch; W.L. Gore and Associates, Inc., Flagstaff, AZ, USA) was prepared which measured 45 mm in length, 25 mm in width, and 0.6 mm in thickness. A partially occluding Satinsky clamp was placed across the RVOT, incorporating the pulmonary annulus (Fig. 1A). Following a period of observation to ascertain that the animal had remained hemodynamically stable, the RVOT was incised along its length, with the pulmonary annulus at the midpoint of this incision; one complete pulmonary valve leaflet was then excised. The patch was then sutured to the edges of the incised RVOT, using a 6-0 running monofilament suture. The clamp was partially released and additional hemostatic stitches placed if necessary before the clamp was removed (Fig. 1B).

An epicardial echocardiographic study was then performed to confirm the presence of pulmonary insufficiency, using two-dimensional (2D) color Doppler. The thoracotomy was closed, after which the animal was allowed to awaken, was extubated, and placed in a recovery pen.

### Follow up MRI

Eight weeks later, the animals were re-anesthetized in similar manner as for the baseline MRI study, and the same instrumentation applied. A full hemodynamic catheterization was performed, followed by repeat MRI scanning.

### Phase-contrast MRI methodology

At both baseline and follow up MRI studies, phase-contrast MRI acquisition was applied at the main and branch pulmonary arteries, and at the aorta for flow quantification. The imaging parameters were: echo time 3.5 ms, three segments, temporal resolution 40 ms, flip angle 25°, matrix of 256 × 128, and voxel size of 2.0 × 1.5 × 5.0 mm (slice thickness) with a resulting signal-to-noise ratio (SNR) of approximately 1.0. Using cardiac gating facilitated by the high-fidelity LV pressure transducer, four averages were obtained for improving the SNR and mitigating against respiratory artifact. The velocity limit was set initially at 150 cm/s, and increased as necessary to accommodate any increased flow velocities. The phase-contrast MRI data analysis involved contouring regions of interest throughout all phases of the cardiac cycle. Forward, regurgitant, and net flows were then automatically calculated from the resulting flow-time curves. The regurgitant fraction (RF) through a region of interest was defined as: RF = (reverse flow/forward flow) × 100. Fractional branch PA pulmonary blood flow (PBF) distribution was calculated as: Fractional branch PA PBF = (net branch PA flow/net total PBF) × 100. Indexed values were obtained by calculating the animal's body surface area (BSA), based on an accepted conversion formula for sheep: [BSA ($m^2$) = 0.097 × weight (kilograms)$^{0.656]}$ (26).

### Ventricular volume analysis

Cine short-axis imaging of the ventricles was acquired from base to apex of the heart using eight contiguous slices of 6-8 mm thickness, depending on the heart size. The RV and LV systolic function analysis involved contouring the blood pool at end-diastole and end-systole at each level of the volume data set, thereby quantifying the end-diastolic volume (EDV) and end-systolic volume (ESV). The stroke volume was defined as the difference between the EDV and ESV, and the ejection fraction (EF) as stroke volume/EDV × 100.

### Euthanasia and post-mortem examinations

Following the terminal MRI scan, the animals were returned to the operating room and, under continuing full general anesthesia, underwent a sternotomy. The heart and great vessels were dissected free from any adhesions, the great vessels clamped, and potassium (100 mEq) administered into the aortic root to arrest the heart. The heart was then excised and the RVOT opened to inspect the technical result of the surgery.

## Results

Using 2D color-flow Doppler echocardiography, all animals were shown to have pulmonary insufficiency immediately after pulmonary valvectomy and transannular patching of the RVOT (Fig. 2). All five animals survived the surgical procedure and completed the study protocol. One animal developed respiratory distress and required anesthesia and ultrasound-

guided drainage of an 800 ml serosanguinous left-sided pleural effusion on postoperative day 18, but remained well thereafter.

The mean body weight at the time of surgery was 69.8 ± 12.4 kg, and at the eight-week MRI scan was 68.4 ± 13.3 kg (p = 0.62). Details of baseline and terminal hemodynamics are listed in Table I. The mean right atrial pressure rose from 7.0 ± 2.0 mmHg at baseline to 18.2 ± 2.5 mmHg at follow up (p <0.001), while the mean diastolic RV pressure rose from 3.3 ± 5.5 mmHg to 15.6 ± 4.8 mmHg at follow up (p = 0.014). The mean diastolic pulmonary artery pressure rose from 11.7 ± 3.8 mmHg at baseline to 18.4 ± 1.7 mmHg at follow up (p = 0.024). The mean LV diastolic pressure was increased significantly at follow up (10.3 ± 5 mmHg versus 19.4 ±1.9 mmHg; p = 0.022).

The mean RF in animals at baseline was 0 ± 0%, and at follow up scanning eight weeks after valvectomy was 37 ± 3% (p <0.001; Fig. 3). The indexed RVEDV was increased from 49 ± 4.0 ml/$m^2$ to 80 ± 10.3 ml/$mm^2$ at follow up (p = 0.01; Fig. 4). The indexed RVESV increased from 13 ± 3.4 ml/$m^2$ to 33 ± 8.8 ml/$m^2$ at follow up (p = 0.01). At baseline, the mean indexed RVSV was 36 ± 3.7 ml/$m^2$, but at post-valvectomy follow up scanning was 47 ± 1.7 ml/$m^2$ (p = 0.01). The mean EF at baseline was 74 ± 6%, and this decreased to 59 ± 5% at follow up (p = 0.02; Fig. 3). The LVEF was also significantly decreased, from 67 ± 2% at baseline to 49 ± 10% at follow up (p = 0.01; Fig. 5).

At post-mortem examination, it was confirmed in all animals that at least one complete pulmonary valve leaflet had been excised. The remaining two leaflets in a typical specimen are shown in Figure 1C.

## Discussion

Patients who have undergone transannular patch repair of ToF during infancy are left with a free pulmonary valve insufficiency, and often have extremely dilated RVOTs. To date, purely percutaneous approaches to valve replacement have not been applicable in such cases (16,20,27), and consequently there is much interest in developing devices and strategies to treat these complex issues via a transcatheter approach (28,29). Whilst preclinical testing in an animal model is a vital component of this developmental process, standard large-animal models do not reflect the harsh anatomic sequelae of repaired congenital heart disease in humans. Hence, a novel device or therapeutic strategy may function well in an animal with a normal, symmetrical RVOT, but fail when faced with the anatomic heterogeneity seen clinically. For this reason, preclinical testing in an animal model that mimics human disease would enhance the design process considerably. Although such animal models have been reported previously, their hemodynamic and remodeling characteristics have not been fully assessed and documented (30-32).

By using cardiac MRI to describe the specific physiological and anatomic consequences associated with transannular patch surgery, a valuable tool has been developed for exploring new approaches to this complex issue. Through paying rigorous attention to the above-described surgical and imaging protocols, RVOT dysfunction and distortion was created reproducibly in the five animals studied which was very similar to that encountered in

human patients with chronic PI. Furthermore, cardiac MRI was used to quantify the changes seen. The extent of PI, as determined with MRI, was severe and consistent in all five animals (mean pulmonary RF 37 ± 3%), and its negative effect on biventricular size and function was dramatic (see Figs. 4 and 5, which show the EFs for the right and left ventricles at baseline and eight weeks after pulmonary valvectomy and transannular patch repair). By using this model, the extent of PI, its effects on RV and LV function, and the time course for the development of these changes, can now be predicted. Moving forwards, this model provides the foundation for the exploration of novel transcatheter devices and of innovative approaches to the treatment of PI.

*In conclusion*, there is today an increasing interest in the field of percutaneous intervention for valvular heart disease, as exemplified by the widespread adoption of transcatheter aortic and pulmonary valve replacement. The pulmonary valve incompetence seen after ToF repair remains clinically challenging to treat. Moreover, the model of PI and dilated RVOT described here may be used for further investigation into the pathophysiologic consequences of these abnormalities themselves, and of any novel intervention proposed in an era of rapidly advancing therapeutic options. This includes devices designed specifically for deployment into the dilated RVOT, or for implantation elsewhere in the pulmonary arterial tree (28,29). Further studies of these devices and approaches in an anatomically appropriate preclinical model, as described in the present study, are required to evaluate the durability of novel devices/approaches and their impact on RV remodeling.

## Acknowledgments

These studies were supported by grants from the National Heart, Lung and Blood Institute of the National Institutes of Health, Bethesda, MD (HL63954 and HL73021), and the American Heart Association, Dallas, TX, USA. R. Gorman and J. Gorman are supported by individual Established Investigator Awards from the American Heart Association, Dallas, TX, USA.

## References

1. Coats L, Tsang V, Khambadkon S, et al. The potential impact of percutaneous pulmonary valve stent implantation on right ventricular outflow tract re-intervention. Eur J Cardiothorac Surg. 2005; 27:536–543. [PubMed: 15784347]
2. Gatzoulis MA, Balaji S, Webber SA, et al. Risk factors for arrhythmia and sudden cardiac death late after repair of tetralogy of Fallot: A multicentre study. Lancet. 2000; 356:975–981. [PubMed: 11041398]
3. Bove EL, Byrum CJ, Thomas FD, et al. The influence of pulmonary insufficiency on ventricular function following repair of tetralogy of Fallot. Evaluation using radionuclide ventriculography. J Thorac Cardiovasc Surg. 1983; 85:691–696. [PubMed: 6843149]
4. Bove EL, Kavey RE, Byrum CJ, Sondheimer HM, Blackman MS, Thomas FD. Improved right ventricular function following late pulmonary valve replacement for residual pulmonary insufficiency or stenosis. J Thorac Cardiovasc Surg. 1985; 90:50–55. [PubMed: 4010322]
5. de Ruijter FT, Weenick I, Hitchcock FJ, Meijboom EJ, Bennick G. Right ventricular dysfunction and pulmonary valve replacement after correction of tetralogy of Fallot. Ann Thorac Surg. 2002; 73:1794–1800. [PubMed: 12078771]
6. Deanfield JE, McKenna WJ, Presbitero P, England D, Graham GR, Hallidie-Smith K. Ventricular arrhythmia in unrepaired and repaired tetralogy of Fallot. Relation to age, timing of repair, and haemodynamic status. Br Heart J. 1984; 52:77–81. [PubMed: 6743425]

7. Dietl CA, Cazzaniga ME, Dubner SJ, Perez-Balino NA, Torres AR, Favaloro RG. Life-threatening arrhythmias and RV dysfunction after surgical repair of tetralogy of Fallot. Comparison between transventricular and transatrial approaches. Circulation. 1994; 90:II7–II12. [PubMed: 7955286]
8. Gatzoulis MA, Till JA, Somerville J, Redington AN. Mechanoelectrical interaction in tetralogy of Fallot. QRS prolongation relates to right ventricular size and predicts malignant ventricular arrhythmias and sudden death. Circulation. 1995; 92:231–237. [PubMed: 7600655]
9. Harrison DA, Harris L, Siu SC, et al. Sustained ventricular tachycardia in adult patients late after repair of tetralogy of Fallot. J Am Coll Cardiol. 1997; 30:1368–1373. [PubMed: 9350941]
10. Silka MJ, Hardy BG, Menashe VD, Morris CD. A population-based prospective evaluation of risk of sudden cardiac death after operation for common congenital heart defects. J Am Coll Cardiol. 1998; 32:245–251. [PubMed: 9669277]
11. Conte S, Jashari R, Eyskens B, Gewiling M, Dumoulin M, Daenen W. Homograft valve insertion for pulmonary regurgitation late after valveless repair of right ventricular outflow tract obstruction. Eur J Cardiothorac Surg. 1999; 15:143–149. [PubMed: 10219546]
12. Bonhoeffer P, Boudjemline Y, Saliba Z, et al. Transcatheter implantation of a bovine valve in pulmonary position: A lamb study. Circulation. 2000; 102:813–816. [PubMed: 10942752]
13. Bonhoeffer P, Boudjemline Y, Saliba Z, et al. Percutaneous replacement of pulmonary valve in a right-ventricle to pulmonary-artery prosthetic conduit with valve dysfunction. Lancet. 2000; 356:1403–1405. [PubMed: 11052583]
14. Bonhoeffer P, Boudjemline Y, Qureshi SA, et al. Percutaneous insertion of the pulmonary valve. J Am Coll Cardiol. 2002; 39:1664–1669. [PubMed: 12020495]
15. Khambadkone S, Bonhoeffer P. Percutaneous implantation of pulmonary valves. Expert Rev Cardiovasc Ther. 2003; 1:541–548. [PubMed: 15030253]
16. Boudjemline Y, Agnoletti G, Bonnet D, Sidi D, Bonhoeffer P. Percutaneous pulmonary valve replacement in a large right ventricular outflow tract: An experimental study. J Am Coll Cardiol. 2004; 43:1082–1087. [PubMed: 15028370]
17. Khambadkone S, Bonhoeffer P. Nonsurgical pulmonary valve replacement: Why, when, and how? Catheter Cardiovasc Interv. 2004; 62:401–408. [PubMed: 15224313]
18. Khambadkone S, Coats L, Taylor A, et al. Percutaneous pulmonary valve implantation in humans: Results in 59 consecutive patients. Circulation. 2005; 112:1189–1197. [PubMed: 16103239]
19. Khambadkone S, Bonhoeffer P. Percutaneous pulmonary valve implantation. Semin Thorac Cardiovasc Surg Pediatr Card Surg Annu. 2006:23–28. [PubMed: 16638543]
20. Khambadkone S, Nordmeyer J, Bonhoeffer P. Percutaneous implantation of the pulmonary and aortic valves: Indications and limitations. J Cardiovasc Med (Hagerstown). 2007; 8:57–61. [PubMed: 17255818]
21. Coats L, Bonhoeffer P. New percutaneous treatments for valve disease. Heart. 2007; 93:639–644. [PubMed: 17435075]
22. McElhinney DB, Hellenbrand WE, Zahn EM, et al. Short- and medium-term outcomes after transcatheter pulmonary valve placement in the expanded multicenter US melody valve trial. Circulation. 2010; 122:507–516. [PubMed: 20644013]
23. Zahn EM, Hellenbrand WE, Lock JE, McElhinney DB. Implantation of the melody transcatheter pulmonary valve in patients with a dysfunctional right ventricular outflow tract conduit: Early results from the U.S. Clinical trial. J Am Coll Cardiol. 2009; 54:1722–1729. [PubMed: 19850214]
24. Coats L, Khambadkone S, Derrick G, et al. Physiological consequences of percutaneous pulmonary valve implantation: The different behaviour of volume- and pressure-overloaded ventricles. Eur Heart J. 2007; 28:1886–1893. [PubMed: 17595193]
25. Mollet A, Basquin A, Stos B, Boudjemline Y. Off-pump replacement of the pulmonary valve in large right ventricular outflow tracts: A transcatheter approach using an intravascular infundibulum reducer. Pediatr Res. 2007; 62:428–433. [PubMed: 17667853]
26. Berman A. Effects of body surface area estimates on predicted energy requirements and heat stress. J Dairy Sci. 2003; 86:3605–3610. [PubMed: 14672191]
27. Boudjemline Y, Schievano S, Bonnet C, et al. Off-pump replacement of the pulmonary valve in large right ventricular outflow tracts: A hybrid approach. J Thorac Cardiovasc Surg. 2005; 129:831–837. [PubMed: 15821651]

28. Capelli C, Taylor AM, Migliavacca F, Bonhoeffer P, Schievano S. Patient-specific reconstructed anatomies and computer simulations are fundamental for selecting medical device treatment: Application to a new percutaneous pulmonary valve. Philos Trans A Math Phys Eng Sci. 368:3027–3038. [PubMed: 20478919]

29. Schievano S, Taylor AM, Capelli C, et al. First-in-man implantation of a novel percutaneous valve: A new approach to medical device development. EuroIntervention. 2010; 5:745–750. [PubMed: 20142228]

30. Kaltman JR, Gillespie MJ, Seymour T, et al. Substrate characterization of ventricular tachycardia in a porcine model of tetralogy of Fallot using noncontact mapping. Pacing Clin Electrophysiol. 2007; 30:1316–1322. [PubMed: 17976092]

31. Petit CJ, Gillespie MJ, Harris MA, et al. Relief of branch pulmonary artery stenosis reduces pulmonary valve insufficiency in a swine model. J Thorac Cardiovasc Surg. 2009; 138:382–389. [PubMed: 19619782]

32. Basquin A, Pineau E, Bonnet D, Sidi D, Boudjemline Y. Transcatheter valve insertion in a model of enlarged right ventricular outflow tracts. J Thorac Cardiovasc Surg. 2010; 139:198–208. [PubMed: 19709678]

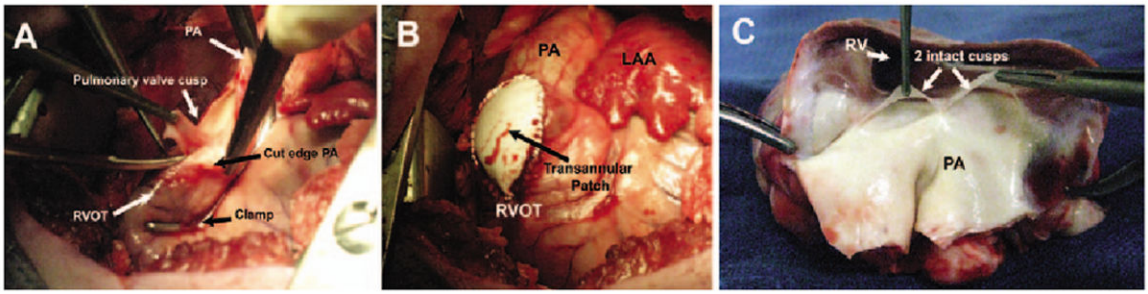


**Figure 1.**

Operative and post-mortem anatomy. A) Intraoperative image of pulmonary valvectoamy, demonstrating a partially occlusive Satinsky clamp across the RVOT/pulmonary annulus. The pulmonary artery has been opened and a pulmonary valve leaflet is being excised. B) Intraoperative image of the completed transannular patch repair. C) Post-mortem specimen of an excised heart from one of the study animals. The RVOT/PA have been laid open by a longitudinal incision through the PA/patch/RVOT, showing thai there only two pulmonary valve leaflets remain intact. LAA: Left atrial appendage; PA: Pulmonary artery; RV: Right ventricle; RVOT: Right ventricular outflow tract.

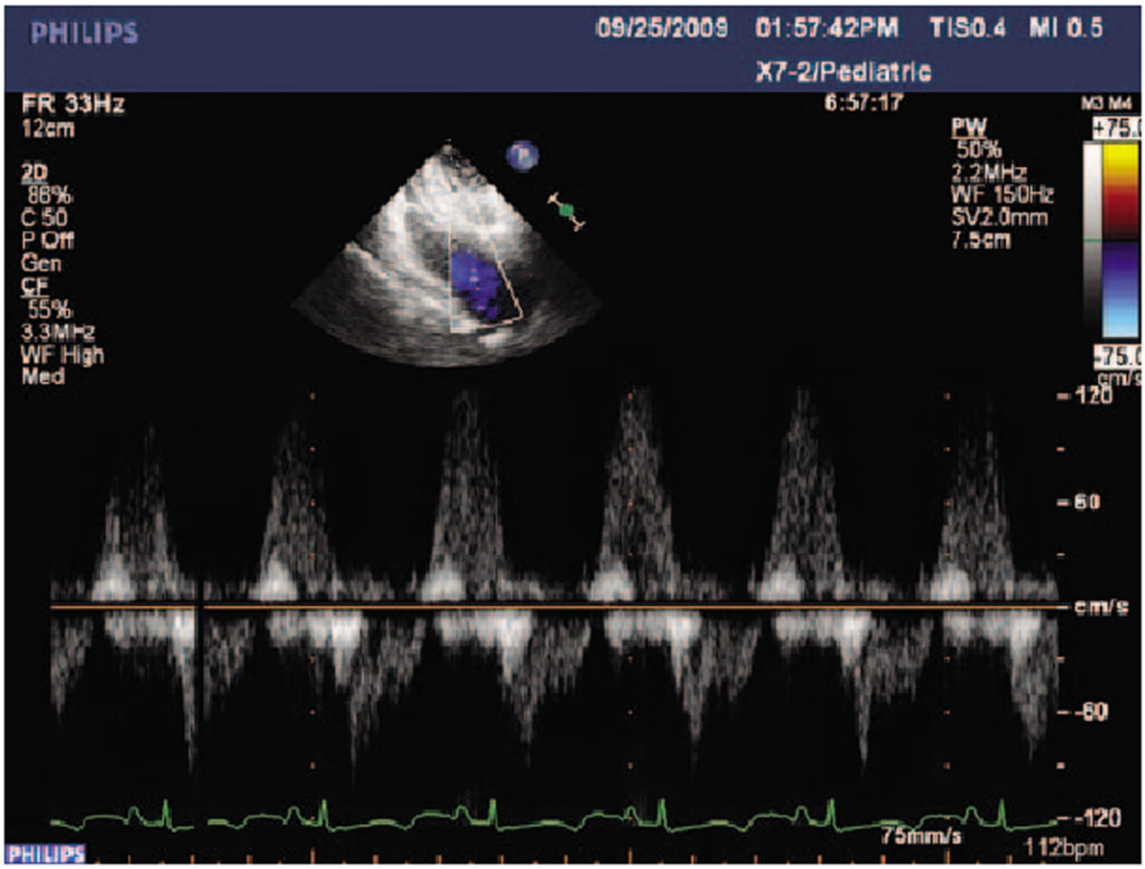


**Figure 2.**

Post-valvectomy pulsed-wave Doppler echocardiographic study demonstrating regurgitant flow in the RVOT at the level of the pulmonary annulus.

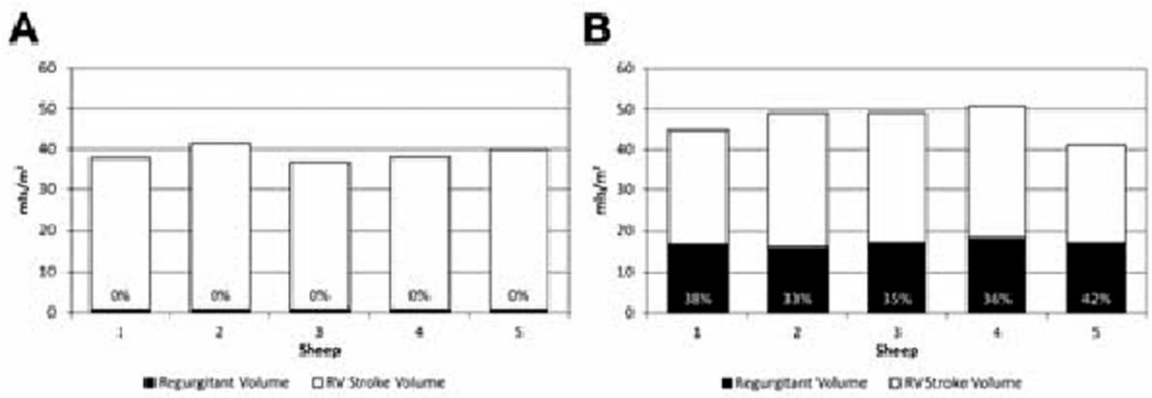


**Figure 3.**

Indexed right ventricular stroke volumes, regurgitant volumes and regurgitant fractions at (A) baseline (n = 5) and (B) at eight weeks after pulmonary valvectomy and transannular patch (n = 5). The regurgitant fractions are expressed as percentages.

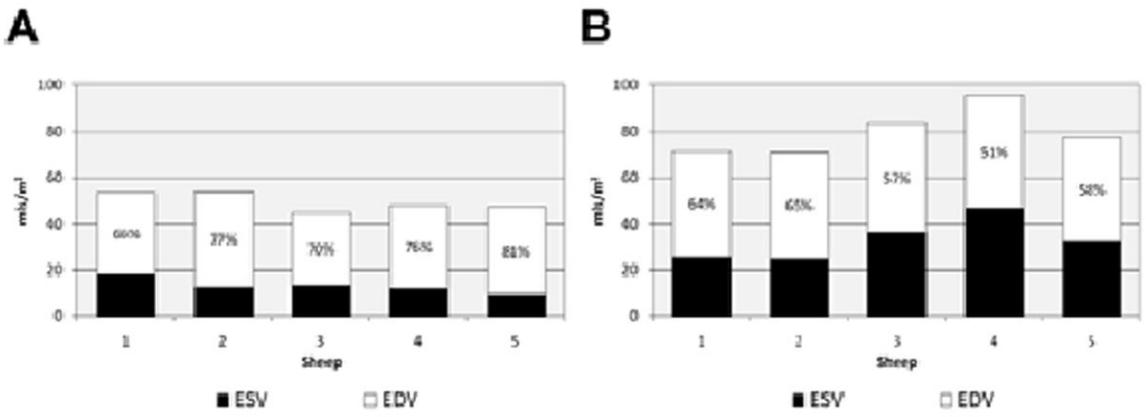


**Figure 4.**

Indexed right ventricular end-diastolic volume (EDV), end-systolic volume (ESV) and ejection fraction at (A) baseline (n = 5) and (B) at eight weeks after pulmonary valvectomy and transannular patch (n = 5). The ejection fractions are shown as percentages.

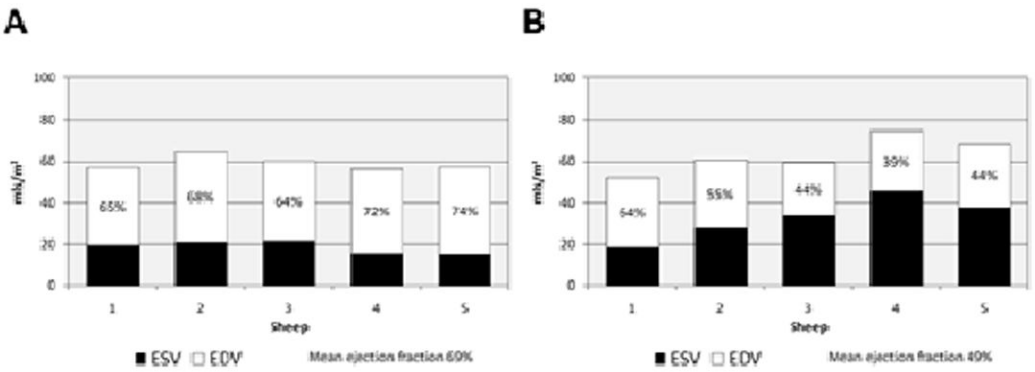


**Figure 5.**

Indexed left ventricular end-diastolic volume (EDV), end-systolic volume (ESV) and ejection fraction at (A) baseline (n = 5) and (B) at eight weeks after pulmonary valvectomy and transannular patch (n = 5). The ejection fractions are shown as percentages.

## Table I

Hemodynamic measurements at baseline and at eight weeks after valvectomy.

| Parameter | Baseline | 8 weeks post-valvectomy | P-value |
|---|---|---|---|
| Body weight (kg) | 69.8 ± 12.4 | 68.4 ± 13.3 | 0.868 |
| Heart rate (bpm) | 100 ± 23 | 105 ± 9 | 0.509 |
| CO (1/min) | 5.0 ± 2.9 | 3.8 ± 1.0 | 0.396 |
| RAP (mmHg) | 7.0 ± 2.0 | 18.2 ± 2.5* | 0.001 |
| Systolic RVP (mmHg) | 26.7 ± 5.9 | 38.2 ± 2.2* | 0.006 |
| Diastolic RVP (mmHg) | 3.3 ± 5.5 | 15.6 ± 4.8* | 0.014 |
| Mean RVP (mmHg) | 12.3 ± 3.2 | 23.6 ± 2.1 | 0.429 |
| Systolic PAP (mmHg) | 23.7 ± 4.7 | 32.8 ± 3.6 | 0.742 |
| Diastolic PAP (mmHg) | 11.7 ± 3.8 | 18.4 ± 1.7* | 0.024 |
| Mean PAP (mmHg) | 16.3 ± 4.9 | 24.6 ± 0.9* | 0.001 |
| Diastolic LVP (mmHg) | 10.3 ± 5.0 | 19.4 ± 1.9* | 0.022 |

All values are mean ± SD.

* Statistically significant versus baseline.

CO: Cardiac output; LVP: Left ventricular pressure; PAP: Pulmonary artery pressure; PCWP: Pulmonary capillary wedge pressure; RAP: Right atrial pressure; RVP: Right ventricular pressure.